

Hugh Summers, Martin O'Mullane, Francisco Guzman, Luis Menchero and Alessandra Giunta

## **Scientific progress report 6**

/today

Workpackages : 8-2, 8-3, 15-1, 15-2, 16-1, 16-2, 16-3, 26-1-6  
Category : DRAFT

This document has been prepared as part of the ADAS-EU Project. It is subject to change without notice. Please contact the authors before referencing it in peer-reviewed literature.  
© Copyright, The ADAS Project.

## **Scientific progress report 6**

Hugh Summers, Martin O'Mullane, Francisco Guzman, Luis Menchero and Alessandra Giunta

Department of Physics, University of Strathclyde, Glasgow, UK

**Abstract:** *The report reviews scientific task completion for project months 31-36*



# Contents

<b>1</b>	<b>Overview</b>	<b>2</b>
<b>2</b>	<b>Individual contributions</b>	<b>3</b>
2.1	Alessandra Giunta: GCR studies	3
2.1.1	Spectral analysis of the solar atmosphere	3
2.1.2	Oxygen analysis	4
2.1.3	GCR developments	4
2.1.4	Transient ionisation in the solar atmosphere	4
2.1.5	MAST Super-X divertor modelling	5
2.2	Hugh Summers: Raising the ADAS GCR baseline to level 1 for medium weight elements	5
2.2.1	Feature emissivities for SANCO and EDGE2D transport codes	5
2.2.2	ADAS database raising to level 1	6
2.2.3	adf04 type conversion	7
2.3	Martin O’Mullane: Code developments and ITER engagements	7
2.4	Francisco Guzmán: Molecular CR modelling	7
2.4.1	ADAS molecular CR modelling time scales generation tool	7
2.4.2	ADAS molecular CR modelling stage 3: adding new data	8
2.4.3	ADAS molecular CR modelling stage 4: population model and CR coefficients	8
2.4.4	Ion impact atomic data	9
2.4.5	ITM collaboration	9
2.5	Luis Menchero: Atomic structure of beam atoms in fields	9
2.6	Nigel Badnell: Electron impact collision cross sections	9
<b>A</b>	<b>ADAS data formats</b>	<b>10</b>
<b>B</b>	<b>PSI 2012 conference submitted abstract</b>	<b>17</b>

<b>C Seminar on MATLAB version of CHEAP code given on November 2011</b>	<b>20</b>
<b>D Experimental quality assessment of Ar CX density profiles</b>	<b>56</b>
<b>E ADAS-EU travel report: ITM workshop Cyprus 3-13 October</b>	<b>64</b>

# **Chapter 1**

## **Overview**

# Chapter 2

## Individual contributions

### 2.1 Alessandra Giunta: GCR studies

This section draws its content from the developments of the research aspects exploited in the Ph.D. thesis “Spectral analysis of the solar atmosphere at the chromosphere-corona boundary”, which has been completed in May 2011. The Ph.D. project was related essentially to an astrophysical context. However, on the atomic side, the development of such a work was designed, within the ADAS environment, to apply to all densities of plasma and was oriented to dynamic conditions. Therefore, it lies in a more general perspective with application not only addressed to astrophysical plasmas but also to those of magnetic confinement fusion devices.

In the following subsection 2.1.1, the thesis work will be outlined, concentrating on the upgrade and advances of the atomic data and modelling adopted. Then four main research fields, which arose from the Ph.D. dissertation, are described in subsections 2.1.2, 2.1.3, 2.1.4 and 2.1.5.

#### 2.1.1 Spectral analysis of the solar atmosphere

The thesis work focussed on developments in atomic modelling and their application to understanding the dynamics of the solar upper atmosphere and the atomic processes involved. The methodology was to use the Generalised Collisional-Radiative (GCR) approach to provide detailed information for most important solar elements, including helium, silicon and iron. These atomic models were used to interpret the UV/EUV spectral measurements from the SoHO/SUMER, SoHO/CDS and Hinode/EIS satellite-based instruments. In particular, the analysis was concentrated on the study of the peculiar behaviour of the intensities of EUV helium lines, as observed by CDS and EIS. Helium exhibits strong emission lines formed in the upper chromosphere/lower transition region. It is however a difficult task to predict their intensities from theory, because of their optical thickness and the long-standing problem of enhancement in their observed line intensities when compared with theoretical intensities. The approach employed in this study was to reconstruct line intensities using Differential Emission Measure (DEM) analysis as diagnostic method, to compare theoretical and observed intensities and evaluate more recent enhancement factors in the optically thin case. As every diagnostic analysis, its reliability is strictly related to the understanding of the underlying atomic physics and the accuracy of the basic and derived atomic data adopted. In such a context, this work aimed to review and update the light and medium weight elements, concentrating on the precision of the previous calculations and performing new calculations to extend and top-up preferred data from literature. In addition, new calculation for silicon ionisation, both for ground to ground and metastable resolved, using the full GCR approach were performed. Because of its low formation temperature ( $\log(T/K) \leq 4.5$ ), a key ion in such an analysis is  $\text{Si}^{+1}$ . From a collisional-radiative point of view and at chromospheric density, this places the problem in a finite density regime leading to redistribution amongst excited states and reducing the effective recombination (especially the dielectronic part of it), due to re-ionisation of excited states.

The careful revisit of atomic data and the new ionisation calculation for silicon gave more accurate results when theoretical and observed line intensities were compared. In particular this leads to two main subsequent work tasks



developed during the six month period and described in the following two subsections (2.1.2 and 2.1.3).

### 2.1.2 Oxygen analysis

The recommendation of atomic data and model with appropriate accuracy was very important to avoid interpretation errors and solve a discrepancy of a factor 2-5 between observed and theoretical intensity line ratio for O IV I(787.7 Å)/I(279.9 Å), reported by Muglach et al. (2010). The source of inconsistency was found to be the incomplete atomic data used to calculate the intensity of the O IV 279.9 Å line. The theoretical line ratio examined by Muglach et al. (2010) showed a significant deviation from the observed ratio, caused by the insufficient number of transitions included in their atomic model. The additional transitions, taken from the distorted wave (DW) calculations of Sampson collected in the ADAS database and included in the revised data, resulted in a decrease of the theoretical line ratio compared to that of Muglach et al. (2010), providing a good agreement with observations. This result was confirmed by a comparison with the recent calculation for O IV of Aggarwal & Keenan (2008). It was also supported by the analysis of three further line ratios originated from the same ion, reflecting the consistency of the atomic dataset used. This work on oxygen has been completed and ended in a forthcoming paper, "Comparison between observed and theoretical O IV line ratios in the UV/EUV solar spectrum as derived by SUMER, CDS and EIS", accepted by Astronomy & Astrophysics on 12 December 2011.

### 2.1.3 GCR developments

The implementation of GCR modelling for Si gave the basis for the extension of this work to the elements beyond Ne. The ionisation and recombination coefficients are supplied within ADAS in the *adf11* data format collections, which are distinguished by different year numbers. The most comprehensive collection available is designed by the mnemonic "89". This is the baseline, but often it is not at the high precision requested in many field related to the high resolution spectroscopy which involve the light and medium-weight elements (i.e. up to Zn). The most accurate GCR ionisation and recombination coefficients are collected under the mnemonic "96", but they are still available only for selected ion, including H, He, C, N, O, Ne. This explains the importance of the GCR extension. New data for Si are now ready and the work is in progress to include all ions of all elements up to Argon, as primary step. The following step will be the extension for elements beyond Ar, possibly up to Zn. This work includes, as a relevant part, the tasks carried out by Professor Hugh Summers, as illustrated in section 2.2.

Another key aspect gathered by the PhD thesis but that exceeded the immediate requirements of an usual solar analysis based on DEM is the independent treatment of metastable states and the whole finite density approach. This is in fact a core assumption of DEM analysis that contribution functions are calculated in ionisation equilibrium. However in a dynamic plasma the ionisation state and possibly excited population state is not relaxed to local thermal conditions. In that context, the role of metastable states, which are handled on the same footing as ground states allowing for slowly relaxing populations, may become essential to understand the measured emission. This aspect converges to two further work projects carried out during the six months period and still in progress, as summarized in the following subsections (2.1.4 and 2.1.5).

### 2.1.4 Transient ionisation in the solar atmosphere

The first project, in collaboration with the Armagh Observatory, concerned the investigation of the role of transient ionisation on the enhancement of the O V 1372 Å line emission during a solar flare occurred on 2 November 1980 (Poland et al., 1984) and the correlation with the hard X-ray emission. The basic model adopted was the one of non-thermal electron beam. This model assumes that electrons are accelerated near the top of a flaring loop. Then the electron beam propagates downward toward the lower atmosphere up to the feet of the loop, where collides with the surrounding protons producing HXR emission and heating the plasma to transition region temperatures. This results in the O V emission. Such a model can explain in principle the observed relationship between the O V and HXR bursts (Cheng et al., 1988) and their overall behaviour. However, difficulties are found in the explanation of the enhanced strength and time profile of the O V emission. The main goal of this work was the analysis of the effects of the plasma not being in ionisation equilibrium due to the rapid heating (that is faster than ionisation/recombination timescales). The issue was addressed considering each burst as an independent entity, which was assumed to originate

as a consequence of the plasma heating at the feet of a single loop in a multiple loop structure. The result was that even a small departure from ionisation equilibrium can explain the enhancement of the O V 1371 Å line emission compared to the intensity calculated in ionisation equilibrium. However some issues have still to be clarified, because this result was based on one flare observation only. More observations together with a statistical analysis are needed to investigate consistently the electron temperature behaviour.

### 2.1.5 MAST Super-X divertor modelling

The second project is an extension of the previous transient study to the interpretation of data from B2-SOLPS simulations in the context of MAST Super-X divertor upgrade. The parallel advance of these two projects underlines the close connection between the astrophysical and laboratory plasmas and clear similarities which allow the development of common modelling approaches. The starting requirement was a prediction of the ionisation state and emission of light impurities helium, carbon and oxygen in a proposed Super-X divertor configuration. From a spectral point of view, the basis for this prediction was a set of values of electron temperature, electron density, ion temperature and neutral hydrogen density on a 2-d poloidal grid in flux surface geometry from the SOLPS code. Firstly, static situations were analysed and the impurity transport was ignored in the atomic model, evaluating local equilibrium ionisation state as a balance of finite-density collisional-radiative ionisation and recombination, as collected in *adf11* ADAS data format. Local emissivity of He I lines in the visible, namely He I 6680 Å, 7067 Å and 7283 Å, is obtained by combining the local emissivity coefficients, available from ADAS *adf15* datasets, with the ionisation fractional abundances and local electron density. A sample of line-of-sight emissivities were provided as quadratures of the local emission. The study was extended to analyse the time evolution of atomic states and spectra during a simple transient model, i.e. an ELM. It was assumed that the density did not change during the transient to assess the influence of a heat pulse propagating through the plasma on the He I and He II emission. The preliminary results showed a possible response of transient for both He I and He II emission to be verified, by comparison with the equilibrium case.

## 2.2 Hugh Summers: Raising the ADAS GCR baseline to level 1 for medium weight elements

The ADAS *baseline* database for arbitrary (especially) heavy elements for collisional-radiative (CR) modelling adopts plane-wave Born (PWB) collisional data calculated in-house by the local ADAS Project. For the important light elements up to silicon, the database has been lifted to *level 2* to support generalised-collisional-radiative (GCR) modelling (see section 2.1.3). Level 2 adopts mostly R-matrix (RM) collisional excitation data obtained from best sources, much of which is, in fact, in-house from the extended ADAS/ADAS-EU Project partnerships. An objective is to raise the ADAS baseline to *level 1* for intermediate weight species, up to zinc, with immediate focus on the the range up to argon. Level 1 adopts distorted wave (DW) for collisional cross-sections and does support GCR modelling. Additionally, level 1 seeks to have consistency in DW usage across recombination and ionisation as well as excitation. The progress, in this time period, is reviewed in sub-section 2.2.2. Other work has concerned theoretical feature emissivity coefficients for 1-d and 2-d JET transport modelling codes (sub-section 2.2.1) and the refreshing of Maxwellian and non-Maxwellian averaging of electron impact cross-sections for large scale conversion of ADAS *adf04* datasets between cross-section and collisional-rate types.(subsection 2.2.3). The following subsection sequence is chronological.

### 2.2.1 Feature emissivities for SANCO and EDGE2D transport codes

It has been the practice for the JET transport codes to use stand-alone Fortran subroutines to access ADAS spectral line photon emissivity coefficients (*pec*). The ADAS data format is *adf15* and the stand-alone access routine is *spec.for*. An additional subroutine *xxspec.for* allows setting of pathways to alternative *adf15* library datasets of different users - other than central ADAS. Reference to specific emissivities required for spectral prediction within the transport code packages is via a look-up table of pathways to the appropriate ADAS *adf15* dataset and index numbers of the required transition within the dataset. The look-up table required refreshing in preparation for the JET EP2 upgrade. Besides including more recent data on light elements it was also necessary to extend the table to spectrum lines of tungsten. For complex systems, such a tungsten, with many ions and large numbers of spectrum lines associated with each ion,

ADAS has implemented a new concept of the feature emissivity coefficient (*fpec*). It is defined for an ion over the pixellated spectral range of a spectrometer and each includes all lines in the wavelength range. In all other respects they are as emissivity coefficients, that is collisional-radiative coefficients which are functions of electron temperature and density. ADAS archives such data in format *adf40*. New Fortran subroutines called *sfpec.for* and *xxsfpec.for* have been written and verified. These are again stand-alone subroutines for use by the JET transport codes. Look-up tables have been updated and the *pec* and *fpec* references for tungsten included. Summers worked with Lauro-Taroni (seconded to JET from RFX Padua) on this task, with Summers handling the ADAS coding and Lauro-Taroni the transport code look-up tables.

## 2.2.2 ADAS database raising to level 1

This development has been possible because Badnell has now made available an extension of his AUTOSTRUCTURE code which evaluates DW collision cross-sections (see ADAS-EU report ECWP1). This extension executes an atomic structure calculation in *ls* and/or *ic* coupling and delivers as output a fully formed ADAS *adf04 type 5* specific ion file. The type 5 dataset has transition lines composed of collision strengths as a function of final state electron energy. A conversion code is also available (see section 2.2.3 below) to convert the type 5 dataset into an *adf04 type 3* data set suitable for thermal plasma GCR population modelling. Badnell has also completed a further extension which allows delivery of an ADAS *adf04 type 6* dataset. The type 6 dataset has transition lines composed of partial collision strengths at threshold energy as a function of incident electron orbital quantum number *l*. This data class provides the input to a economised route to calculation of dielectronic recombination (DR) called the Burgess Bethe General Program (BBGP) method. This method, simpler than the full AUTOSTRUCTURE calculation of DR, maintains the DW consistency stated in the introduction to section 2.2 but is compact enough to allow progress through ions with occupied M and N shells, as required here. Summers worked with Badnell to tune the AUTOSTRUCTURE DW output to precise ADAS specifications. Special attention was given to adjusting field lengths appropriately for the long configuration strings of the more complex ions, to ensuring correct inclusion of the orbital energy list and to settings ensuring consistency of orbital energies between *ls* and *ic* calculations. Other small issues and adjustments included numerical start up of radial wave functions in a kappa averaged potentials. These details were important, since it also means that baseline *adf04* PWB datasets can be merged safely with *adf04* DW datasets. This is a practice necessary when DW calculations become excessively large.

It was decided to set the processing up as a semi-automatic, large scale arrangement under offline-ADAS, using driver datasets and distributed processing of complete iso-electronic sequences at a time. Since ADAS series 7 has historically been associated with AUTOSTRUCTURE calculations and postprocessing, it was appropriate to assign *././offline\_adas/adas7#3/* to the development with PERL scripts in the sub-directory */scripts* controlling events. ADAS uses format *adf27* for AUTOSTRUCTURE drivers and it was convenient to continue with this practice, but with tightly prescribed naming conventions and sub-directory structures. Thus

```
././adf27/dw/ < isoseq > like/cophps# < isoseq > | < coupling > # < elemsym > < ioncharge > .dat
```

has the DW drivers. It is noted that other outer directories *././adf27/pwb/* and *././adf27/dw\_bbgp/* in a similar manner handle PWB and BBGP drivers for AUTOSTRUCTURE. Summers has set up the following scripts:

1. *adas7#3\_dw\_bbgp\_llbatch.pl*
2. *adas7#3\_dw\_llbatch.pl*
3. *adas7#3\_pwb\_llbatch.pl*
4. *process\_ion\_dw\_adf27\_to\_adf04.pl*
5. *process\_ion\_dw\_bbgp\_adf27\_to\_adf04.pl*
6. *process\_ion\_pwb\_adf04\_t1\_to\_adf04\_t3.pl*
7. *process\_ion\_pwb\_adf27\_to\_adf04.pl*
8. *process\_isoseq\_dw\_adf04\_t5\_to\_adf04\_t3.pl*
9. *process\_isoseq\_pwb\_adf04\_t1\_to\_adf04\_t3.pl*
10. *process\_isoseq\_pwb\_dw\_adf04\_merge.pl*

11. setup\_isoseq\_dw\_adf27.pl
12. setup\_isoseq\_dw\_bbgp\_adf27.pl
13. setup\_isoseq\_pwb\_adf27.pl

The script names are mostly self-explanatory. Scripts 11-13 prepare the *adf27* drivers for each ion from *ls* and *ic* templates which are set for each isoelectronic sequence. Scripts 12 and 13 require the precalculation of the PWB *adf04* datasets so that correct free electron energy ranges can be derived from them. Scripts 1-3 are the mass production ones which are set currently to initiate distributed processing under LOADLEVELLER on the JAC machines at JET. A typical DW example for the p-like sequence uses ~ 40 machines and the individual calculation on one machine takes ~ 6 days. In the p-like case, the final DW *adf04* dataset is ~ 60 Mbytes spanning ~ 1000 levels in *ic* and including ~ 500,000 transitions. Every ion of iso-electronic sequences H to Ar with members up to element zinc is included. In the present time period, the whole system was set up and around half of the sequences processed. All these codes and scripts will be released in an upcoming ADAS distribution.

### 2.2.3 *adf04* type conversion

The mass processing described in section 2.2.2 includes conversion of ADAS *adf04* datasets of type 1 and 5 (with transition lines tabulations of collision strengths to type 3 (with transition lines tabulations of Maxwell averaged collision strengths (Y). Bryans and Summers, a number of years ago, made a large extension to ADAS allowing it to handle non-Maxwellian distribution functions. That development included a universal convertor which handled arbitrary distribution functions including Maxwellians. With non-Maxwellian distribution functions, the standard *adf04 type 3* dataset is more subtle since up and down rate coefficients cannot be derived via detailed balance and must be separately tabulated. Bryans and Summers called these 'Upsilons' (Y) and 'Downsilons' (J). The original convertor remains in ADAS as code ADAS809. An extracted stand-alone version *adf04\_om2ups.for* was prepared for use in AUTOSTRUCTURE DW post processing, restricted to Maxwellians alone. *adf04\_om2ups.for* behaviour had become discrepant for unexplained reasons. In this time period, Summers re-examined *adf04\_om2ups.for* and its associated sub-routines and isolated the error as due to a change in convention of the signs of the Bethe parameter delivered by AUTOSTRUCTURE to its *adf04 datasets*. Summers corrected these faults, but also brought *adf04\_om2ups.for* back to full non-Maxwellian functionality. This included revision of the primary *adf04* reading routine *xxdata\_04.for* and writing routine *xxwrto\_04.for*. It is anticipated that non-Maxwellians will become an important part of ADAS/ADAS-EU activity in later time periods. These changes will be included in the next ADAS release.

## 2.3 Martin O'Mullane: Code developments and ITER engagements

### 2.4 Francisco Guzmán: Molecular CR modelling

Here will be described status of the work of Dr. Francisco Guzmán over molecular CR modelling and ion-impact data during the period concerning to this report.

#### 2.4.1 ADAS molecular CR modelling time scales generation tool

A new tool called *gettaus* has been embedded in ADAS901 collection of routines has been created. This calculates time scales for the processes stored in either the formats *mdf33*, *mdf34*, *mdf04* or *mdf14*. There are various possibilities:

- Time scales for a set of processes
- Time scales for a set of states
- Time scales for dissociation

In both cases, *gettaus* is looking selecting and calculating maxwellian relaxation times for these processes. Time scales have been calculated and compared for the original data and the result summarized in PUBL6 report (contents in Appendix A). **This work concerns to partial completion of work package task 18-2.**

### 2.4.2 ADAS molecular CR modelling stage 3: adding new data

Original H<sub>2</sub> data sets are not completed. Reaction rates between excited states, ionization rates and dissociative excitation and ionization rates are lacking in the literature. So happens with more complicated diatomic molecules as N<sub>2</sub>.

It is necessary to complete these data with reasonable quality data that could be calculated in a fast and simple way. To achieve this goal impact parameter approximation[?] have been used for those process. In this way a new routine *IPMrate* have been created from the original ADAS *IPrate* adapted to the molecular case. For ionization and dissociation cases central ADAS routine *r8ecip* is used.

In order to obtain the lacking data and merge and organize them with the original rates stored in *mdf33* and *mdf34* formats, program ADAS903 is created. This program looks for the gaps in the matrix and according some rules given in the driver *input903.dat* is calculating the new rates in an automatic way and writing the final *mdf04* file. ADAS903 is respecting the vibrational resolution of the metastables as the CR modelling applies to homonuclear diatomic molecules which have not permanent dipolar moment between vibrational states of the same electronic state so the spontaneous transitions are forbidden. ADAS903 is not calculating ionization to “ordinary” (non-metastable) states as they will be not in competition with ionization to metastables. CR model only consider ionization to metastables. Two types of resolution are allowed here: full vibrational resolution and electronic resolution where vibronic transition are summed over the electronic levels save in metastables.

A new database of dipole probabilities A-values have been put in the *mdf00* directories to be used by ADAS903, *IPMrate* and future routines (e.g. ADAS904 CR model program). Reading routine *xxdatm\_00* that was reading Franck-Condon Factors previously has been modified to read A-values as well as they are in very similar format. ADAS903 is only calculating allowed dipole transitions, for it two files of dipolar transition rules are placed in A-values directories. A new routine called *dgfctr* is correcting these values from the statistical G-factor[?].

In the H<sub>2</sub> case the molecular cation H<sub>2</sub><sup>+</sup> has only one metastable: the ground state; being the others dissociative states. Neutral H<sub>2</sub> has a metastable in the orthohydrogen state *c*<sup>3</sup>Π<sub>u</sub>, but the decay time of this (~ 1ms)[?] is comparable to ion-impact ionization time at low temperatures of the order of 1eV, so transition integrals from Freis *et al.* has been added to *mdf00/aval* directory.

Electronic and vibrational resolution *mdf04* files have been successfully generated from previous *mdf33* files containing all the needed transitions to create a population model. **These is the basis of CR model inside milestone SCI51. This work also concerns to partial completion of work package task 18-1 and 18-2.**

### 2.4.3 ADAS molecular CR modelling stage 4: population model and CR coefficients

The collisional-radiative model for molecules is in developing phase together with the ADAS904 program. The molecular CR model will make use of the calculated rates and the new molecular CR coefficients will be called analogous to the atomic case adding an “M” to distinguish them from the atomic case: MACD for molecular recombination, MCX-IACD for inverse charge exchange, TMACD for the sum of the two previous coefficients, MQCD for the CR excitation coefficients, MSCD for molecular ionization coefficients and MXCD for cross coupling coefficients. in addition to that new coefficients coming from dissociative processes and the need of having an input flux will be provided: MFCD for the molecular input flux, FCD for atomic input flux, FXCD for atomic cross coupling input flux, DCD for dissociative coefficients, PDCD for partial(one molecular ionization stage) compressed dissociative coefficients, TDCD for total compressed dissociative coefficients (from all ionization stages), TXDCD for total cross coupling dissociation coefficients. To these atomic CR coefficients should be added from central ADAS formats to solve the population matrix.

These coefficients together with the equations will be described over the next period in PUBL6 report (Appendix A).

Results will be presented in Plasma Surface Interaction conference which will be held in May 2012 in the city of Aachen, Germany. Abstract is attached in Appendix B. **The completion of the last stage will suppose the completion of work package 18 task (save experimental validation (task 18-4)).**

#### 2.4.4 Ion impact atomic data

Charge exchange recombination spectroscopy is the most direct technique to determine the argon density in a fusion plasma. This technique requires knowledge of the Ar charge-exchange (CX) cross-sections. New calculations of Ar cross-sections using an improved hydrogenic description of the initial distribution [?] (the previous sets come from calculation that used a microcanonical distribution [?]) have been released in ADAS. A big discrepancy has been found between the different calculations reaching up to two orders of magnitude depending on the beam energy.

During the previous period (see science\_5 report) a experiment has been carried in the fusion device Tore Supra where Ar was injected in the vessel during operation. The quality of the CX cross-sections for ArXVIII will be studied by comparing argon density profiles evaluated through CXRS, using both cross-section data-sets, with those evaluated through the combined use of the soft-X Ray (SXR) diagnostic and using transport code ITM managed by collaborator Remy Guirlet. To analyse the CXRS data and obtain the impurity profile from these data CHEAP code will be used. However, the state of CHEAP code version in Tore Supra was not adequate to perform this analysis as it was using old Fortran libraries and using outdated data stored in local files. F. Guzmán has updated the code to a full Matlab version in agreement with the responsible persons for Tore Supra spectroscopy diagnostic and code creator M. von Hellerman. The atomic data used have been updated to central ADAS as well and now a working version is available at Tore Supra. A general seminar was given and is included in Appendix C.

#### ASDEX-U campaign 2012 proposal

In the same topic the necessity of more experimental shots has arrived to the elaboration of a proposal for a dedicated experiment in ASDEX-U. The proposal is included in Appendix D. The experiment has been approved and will be done during the next period.

**The actions 2.4.4 are included in the partial completion of revision of fiducial CXS data (work package task 9-4).**

#### 2.4.5 ITM collaboration

Collaboration with Integrated Tokamak Modelling project is started by means of the participation of Francisco Guzmán in a workshop on October 2011. Agreements of the utilization of molecular data from ADAS molecular CR model have been done. The travel report is attached in Appendix E. **This collaboration will result in the completion of revision task from work packages 17-2 and 18-4.**

### 2.5 Luis Menchero: Atomic structure of beam atoms in fields

### 2.6 Nigel Badnell: Electron impact collision cross sections

## **Appendix A**

### **ADAS data formats**

[1] ADAS-EU/REPORTS\_PUBL/PUBL\_6/ pages 1-6



-

ADAS-EU R(10)PU06

**ADAS-EU**  
ADAS for fusion in Europe

Grant: 224607

---

F. Guzmán

**The Molecular ADAS: Molecular population model for fusion plasmas**

26 July 2010

Workpackages : –  
Category : DRAFT

# **The Molecular ADAS: Molecular population model for fusion plasmas**

F. Guzmán

Department of Physics, University of Strathclyde, Glasgow, UK

**Abstract:** *Public report for ADAS\_EU*

# Contents

<b>1</b>	<b>Introduction</b>	<b>4</b>
1.1	Molecules in plasmas	4
1.2	H <sub>2</sub> System	4
1.3	Isotopic Scaling	4
<b>2</b>	<b>H<sub>2</sub> data</b>	<b>5</b>
2.1	Type of data and quality	5
2.2	Fitting formulas	5
2.3	Scaling and classical models	5
2.3.1	Scaling	5
2.3.2	Classical Models	5
2.4	Maxwell rates	5
2.4.1	Single maxwellian integrations for electron-impact collisions	5
2.4.2	Double maxwellian integrations for ion-impact collisions	5
<b>3</b>	<b>Collisional-Radiative model for molecules</b>	<b>6</b>
3.1	Molecular Generalized Collisional-Radiative Model	6
3.1.1	Time Scales	6
3.2	Vibrational resolution in molecular GCR	10
3.3	Source terms	10
3.4	Other Molecular Collisional-Radiative Models	10
<b>4</b>	<b>ADAS9xx: The molecular ADAS</b>	<b>11</b>
4.1	Structure and Diagrams	11
4.1.1	MDF: The Molecular ADAS format	11
4.1.2	Index of parameters in <i>mdf</i> files	15
4.2	The Molecular ADAS routines	15

4.2.1	Scaling, widening and resolving . . . . .	15
4.2.2	The collisional-radiative routines . . . . .	15
<b>5</b>	<b>Results</b>	<b>16</b>
5.1	Checking in the experimental plasma . . . . .	16
5.2	The molecular challenge. ADAS9xx: a general molecular software . . . . .	16
<b>A</b>	<b>MDF data formats</b>	<b>18</b>
A.1	<i>mdf00</i> : general parameter information files and potentials curves . . . . .	18
A.1.1	potentials . . . . .	18
A.1.2	vibrational energies . . . . .	18
A.1.3	Franck-Condon Factors . . . . .	22
<b>B</b>	<b>IDL procedures</b>	<b>24</b>
<b>C</b>	<b>FORTRAN subroutines</b>	<b>25</b>
C.1	ADAS902 . . . . .	25
C.1.1	adas902.for . . . . .	26
C.1.2	thermrat.for . . . . .	44
C.1.3	intrap.for . . . . .	51
C.1.4	extrap.for . . . . .	55
C.1.5	dstform.for . . . . .	59
C.1.6	wrt_mdf04.for . . . . .	61
C.1.7	fcf.for . . . . .	65
C.1.8	rd_enu.for . . . . .	67
<b>D</b>	<b>Shell scripts</b>	<b>69</b>
<b>E</b>	<b>Fitting Formulas</b>	<b>70</b>



## Appendix B

# PSI 2012 conference submitted abstract

### ADAS Tools for Collisional-Radiative Model for Molecules

F. Guzmán<sup>1,2</sup>, M. O'Mullane<sup>1</sup> and H. P. Summers<sup>1</sup>

<sup>1</sup>*Department of Physics, University of Strathclyde, Glasgow, G1 1XQ, UK.*

<sup>2</sup>*CEA Cadarache, Saint-Paul-lez-Durance, 13108, France.*

Molecules desorbed from the wall are present in the edge of tokamak plasmas – they contribute to the neutral density through dissociation and influence divertor physics through processes such as Molecular Assisted Recombination (MAR) changing neutral population balance. Therefore a complete model of the edge plasma must include molecules and should track the evolution and break-up of these plasma species [1]. Collisional-radiative (CR) coefficients are needed for the interpretation of measurements. Present day simulation codes consider CR coefficients from hydrogen (e.g. [2,3]) and some of the hydrocarbon molecules (e.g. [4]). Under the framework of ADAS-EU project we have developed a CR model for molecules which incorporate vibronic states that can play a significant role in the CR description of the molecular system. A collisional-radiative model for homonuclear diatomic molecules is described. To demonstrate the behaviour of the population model two resolutions are considered: (i) electronic resolution where vibronic transitions are summed over the electronic levels and (ii) full vibrational resolution where the vibrational states are considered individually. Even in the grosser resolution, the vibrational states of the metastables must be treated separately since no spontaneous transitions between them are allowed due to the absence of a permanent dipolar moment. A structured, comprehensive, collection of the fundamental data (which is archived) forms the input to the collisional-radiative population code. A new compilation [5] of the required cross sections has been used to create the input files described for H<sub>2</sub> system. 1665 non-zero transitions in resolution (i) and 35048 in resolution (ii) (electronic levels up to main quantum number N=4) have been considered. New reaction rates between the excited states and between the vibronic levels have been calculated by means of the impact parameter approximation [6] for excitation and ionization. The Franck-Condon regime can be assumed because of the plasma energies typical of edge and divertor. The inclusion of processes from excited states alter the dissociation and ionization coefficients leading to an increase of the neutral atom population: the maxwellian dissociation time constants decrease by a factor of 10 when considering all vibronic states from ground state. New computer tools are presented which enable and simplify this data assembly. For a set of typical plasma edge conditions effective collisional-radiative line/band coefficients are shown and a detailed description of the influence of the metastable's vibronic states on these effective rate coefficients is presented. The difference between the rate coefficients calculated in the full and reduced resolutions forms the basis of an estimation of the precision and recommendations on the level of resolution required for diagnostic and modelling purposes are given.

[1] D. Tskhakaya et al. *Contrib. Plasma Phys.* **48**, 121–125 (2008)

[2] K. Sawada and T. Fujimoto *J. Appl. Phys.* **78**, 2913 (1995)

[3] D. Wunderlich et al. *J. Quant. Spec. Rad. Transfer* **110**, 62–71 (2009)

[4] R.Janev, D.Reiter and U.Samm **Juel-Report 3966, 4005, 4038**

[5] R.Janev, D.Reiter and U.Samm (private communication).

[6] A. Burgess and H.P. Summers *MNRAS* **174**, 345 (1976).

-



## Appendix C


# Seminar on MATLAB version of CHEAP code given on November 2011

New MATLAB version of CHEAP for impurity  
density profiles using CXRS data

Francisco Guzmán

ADAS-EU  
University of Strathclyde  
CEA-Cadarache

November 7, 2011

 1/15

## Outline

- 1 What is CHEAP?
- 2 Working with CHEAP
- 3 INPUT data
- 4 An example: C impurity, # 36074
- 5 Conclusions



## Outline

- 1 What is CHEAP?
- 2 Working with CHEAP
- 3 INPUT data
- 4 An example: C impurity, # 36074
- 5 Conclusions

## Outline

- 1 What is CHEAP?
- 2 Working with CHEAP
- 3 INPUT data
- 4 An example: C impurity, # 36074
- 5 Conclusions

## Outline

- 1 What is CHEAP?
- 2 Working with CHEAP
- 3 INPUT data
- 4 An example: C impurity, # 36074
- 5 Conclusions



## What does CHEAP do?

- $(T_i, T_e, n_e, \phi_{CX})$  profiles  $\implies$  beam density attenuation  $\implies$  calculated photon flux  $\implies$  impurity densities.
- CHEAP can use several background impurities to calculate beam attenuation.
- $q_{eff}(Z, H(n=1, 2))$  CX data is used to calculate beam attenuation.  
 $q_{eff}(n=2)$  CX line emission contribution under implementation.
- $Z_{eff}^{CX}$  could be calculated from impurity profiles and can be implemented.
- A storage of processed data (i.e. impurity density profiles) planned.





## What does CHEAP do?

- $(T_i, T_e, n_e, \phi_{CX})$  profiles  $\implies$  beam density attenuation  $\implies$  calculated photon flux  $\implies$  impurity densities.
- CHEAP can use several background impurities to calculate beam attenuation.
- $q_{eff}(Z, H(n = 1, 2))$  CX data is used to calculate beam attenuation.  
 $q_{eff}(n = 2)$  CX line emission contribution under implementation.
- $Z_{eff}^{CX}$  could be calculated from impurity profiles and can be implemented.
- A storage of processed data (i.e. impurity density profiles) planned.

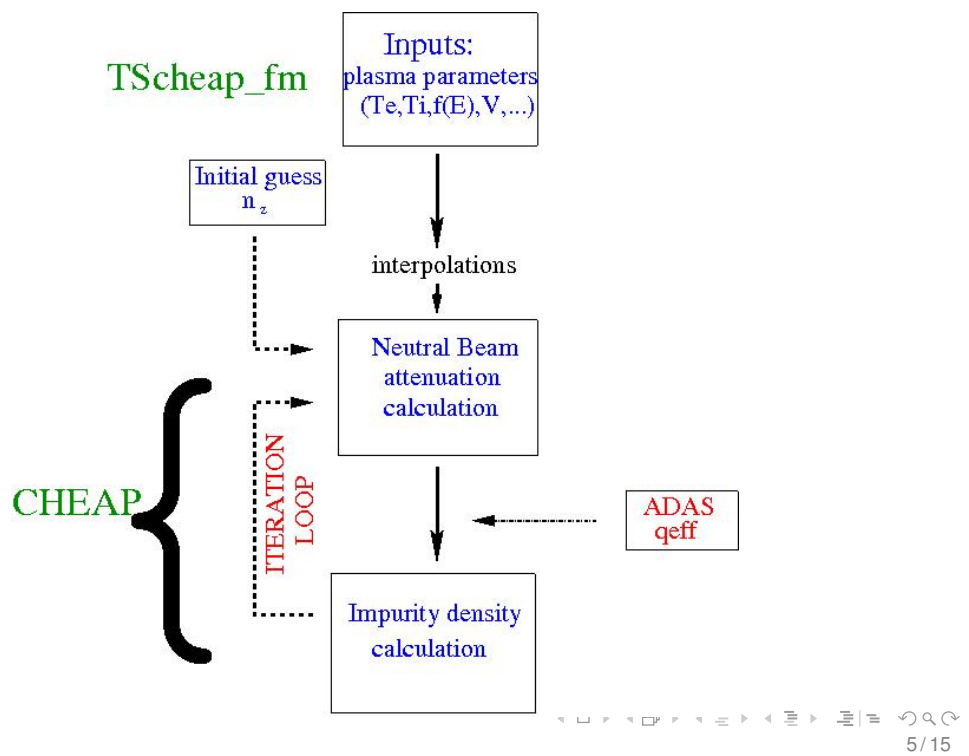
## What does CHEAP do?

- $(T_i, T_e, n_e, \phi_{CX})$  profiles  $\implies$  beam density attenuation  $\implies$  calculated photon flux  $\implies$  impurity densities.
- CHEAP can use several background impurities to calculate beam attenuation.
- $q_{eff}(Z, H(n = 1, 2))$  CX data is used to calculate beam attenuation.  
 $q_{eff}(n = 2)$  CX line emission contribution under implementation.
- $Z_{eff}^{CX}$  could be calculated from impurity profiles and can be implemented.
- A storage of processed data (i.e. impurity density profiles) planned.

## What does CHEAP do?

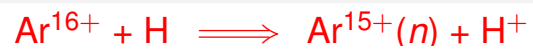
- $(T_i, T_e, n_e, \phi_{CX})$  profiles  $\implies$  beam density attenuation  $\implies$  calculated photon flux  $\implies$  impurity densities.
- CHEAP can use several background impurities to calculate beam attenuation.
- $q_{eff}(Z, H(n=1,2))$  CX data is used to calculate beam attenuation.  
 $q_{eff}(n=2)$  CX line emission contribution under implementation.
- $Z_{eff}^{CX}$  could be calculated from impurity profiles and can be implemented.
- A storage of processed data (i.e. impurity density profiles) planned.

## CHEAP structure

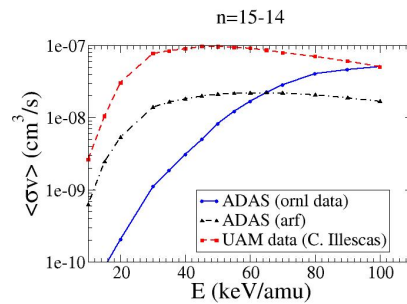
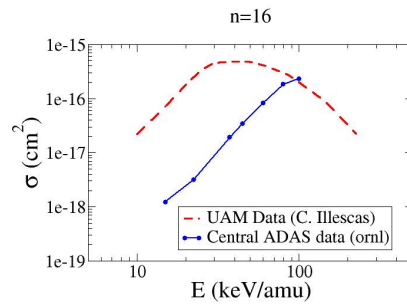


# An use of CHEAP: ADAS sets comparison

Ar<sup>16+</sup> + H



Factor between 5 and 25 of difference in the  $T_i$  relevant ranges.

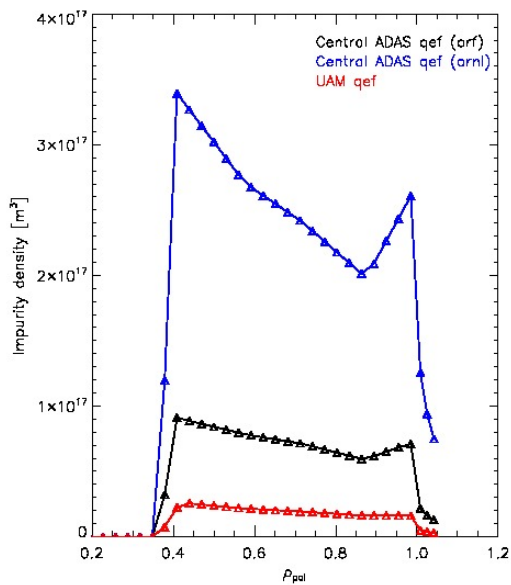


# CXRS Densities from QEF

CHEAP Results from ASDEX-U

## Shot 22305; ArXVI profile

Shot = 22305 Time = 2.650 s



Radial density profile obtained from the fitting of calculated line intensity to the experimental one using the CHEAP code in ASDEX-U.

Data	ORNL	UAM	ARF	X ray
Conc. Ar	0.02123	0.00104	0.00482	0.001

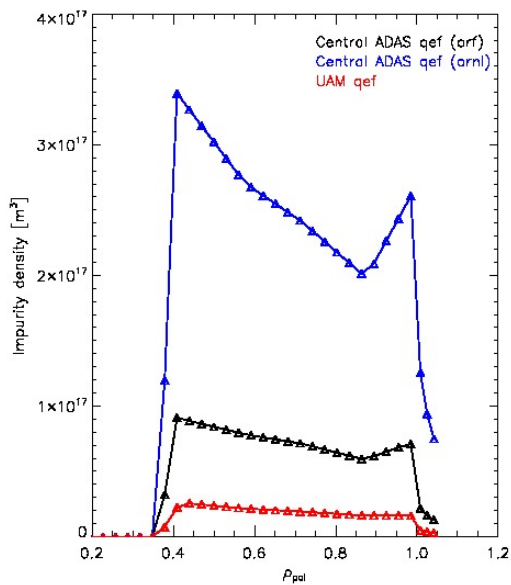
F Guzmán and C. Maggi (Spring 2009).  
X ray data provided by M. Sertoli

# CXRS Densities from QEF

CHEAP Results from ASDEX-U

## Shot 22305; ArXVI profile

Shot = 22305 Time = 2.650 s



Radial density profile obtained from the fitting of calculated line intensity to the experimental one using the CHEAP code in ASDEX-U.

Data	ORNL	UAM	ARF	X ray
Conc. Ar	0.02123	0.00104	0.00482	0.001

UAM data agree with Soft X-ray

F Guzmán and C. Maggi (Spring 2009).

X ray data provided by M. Sertoli



## Plasma parameters

- 1 Pulse number
- 2 Impurity ion H, He, Be, B, C, N,O, Ne or Ar.
- 3 Time index for diagnostic and estimated concentration of background impurities (at the moment C, He,Ne and Ar)
- 4 Energy fractions, voltage, impact parameter and Z of NB.

## Plasma parameters

- ① Pulse number
- ② Impurity ion H, He, Be, B, C, N,O, Ne or Ar.
- ③ Time index for diagnostic and estimated concentration of background impurities (at the moment C, He,Ne and Ar)
- ④ Energy fractions, voltage, impact parameter and Z of NB.

## Plasma parameters

- ① Pulse number
- ② Impurity ion H, He, Be, B, C, N,O, Ne or Ar.
- ③ Time index for diagnostic and estimated concentration of background impurities (at the moment C, He,Ne and Ar)
- ④ Energy fractions, voltage, impact parameter and Z of NB.

## Plasma parameters

- ① Pulse number
- ② Impurity ion H, He, Be, B, C, N,O, Ne or Ar.
- ③ Time index for diagnostic and estimated concentration of background impurities (at the moment C, He,Ne and Ar)
- ④ Energy fractions, voltage, impact parameter and Z of NB.

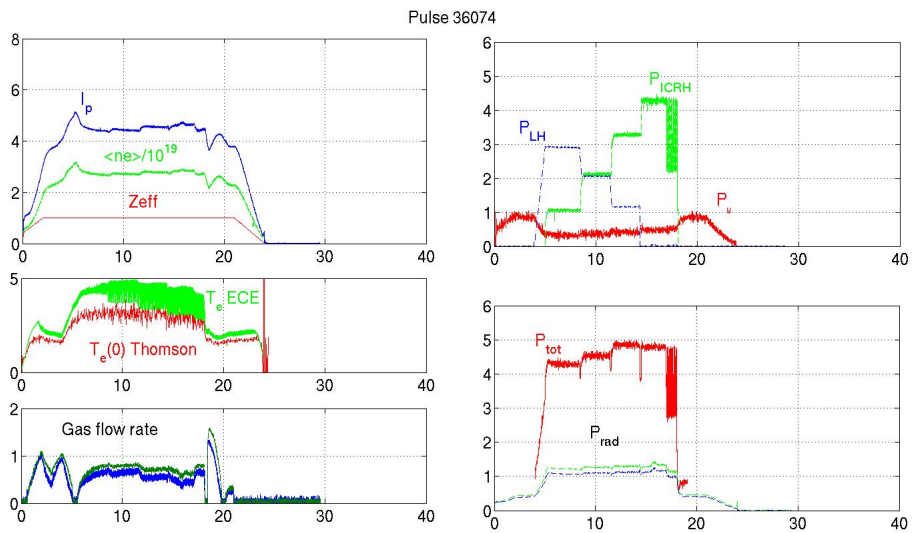
## CXRS and diagnostics

These data are taken from TSBASE and interpolated to the required CX radius values.

- CX line proton  $T_i$  and geometry  $\longleftrightarrow$  CX diagnostic
- NB current  $\longleftrightarrow$  SIDN
- $T_e$   $\longleftrightarrow$  ECE, Thomson scattering and TPROF. Preferred TPROF.
- $n_e$   $\longleftrightarrow$  TPROF, reflectometry or interferometry. Preferred TPROF

An example: C impurity, # 36074

## # 36074 parameters

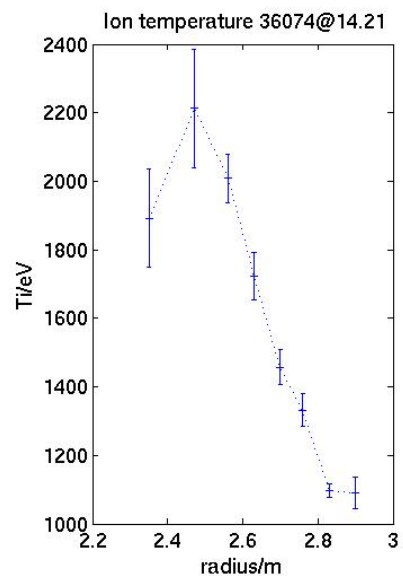
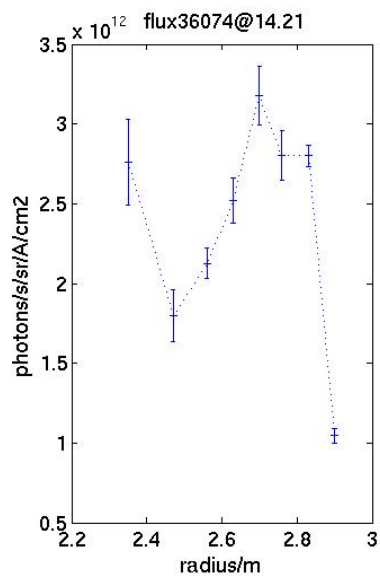


(see also Blassel's internal report 2007)

An example: C impurity, # 36074

## The input flux and $T_i$

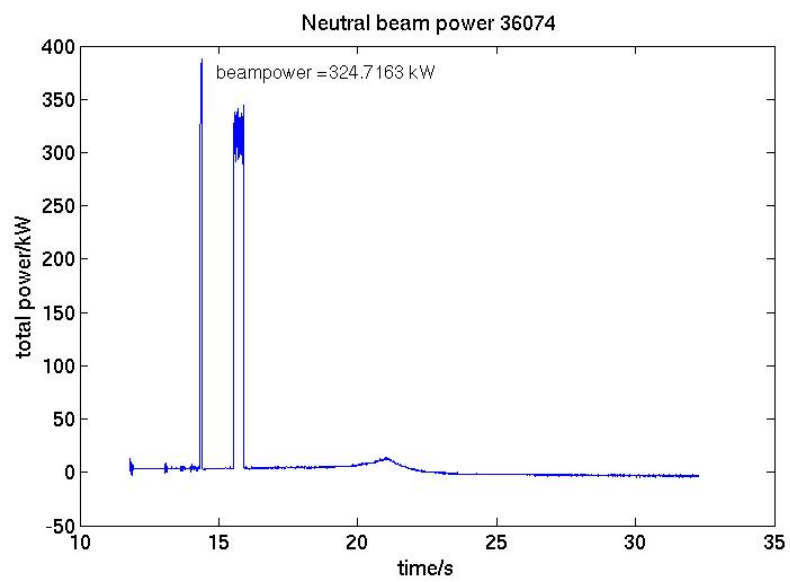
# 36074



An example: C impurity, # 36074

## The NBI power

# 36074

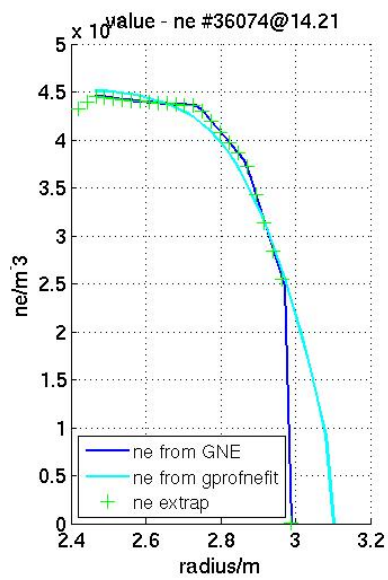
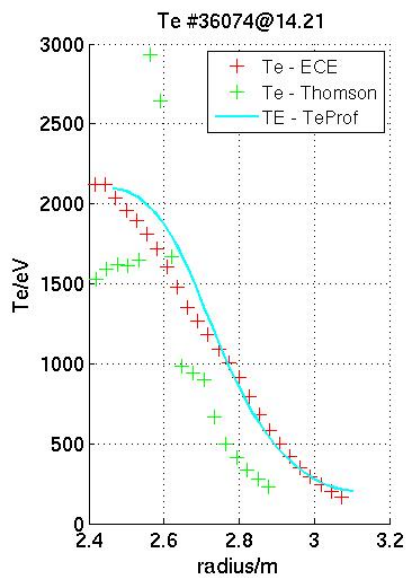




An example: C impurity, # 36074

# The input $T_e$ and $n_e$

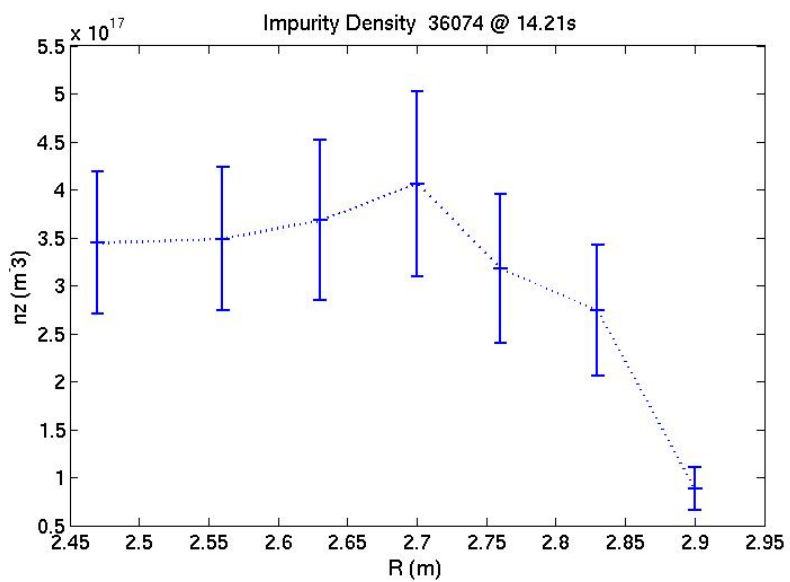
# 36074



An example: C impurity, # 36074

## The resulting profile of CVI

# 36074

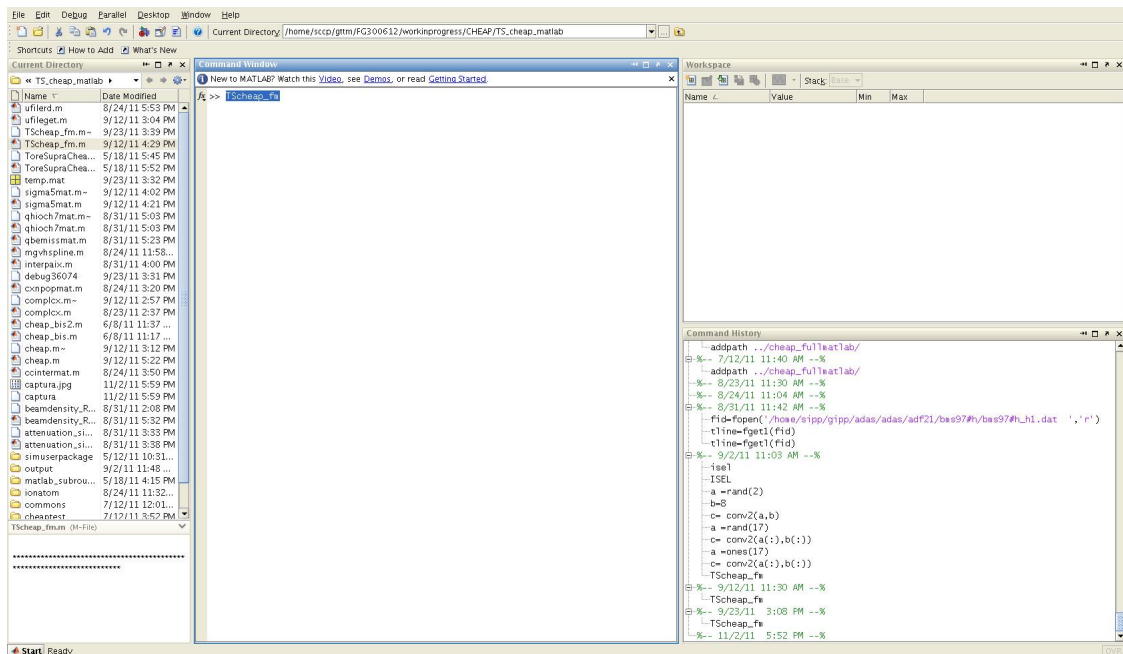


## Conclusions

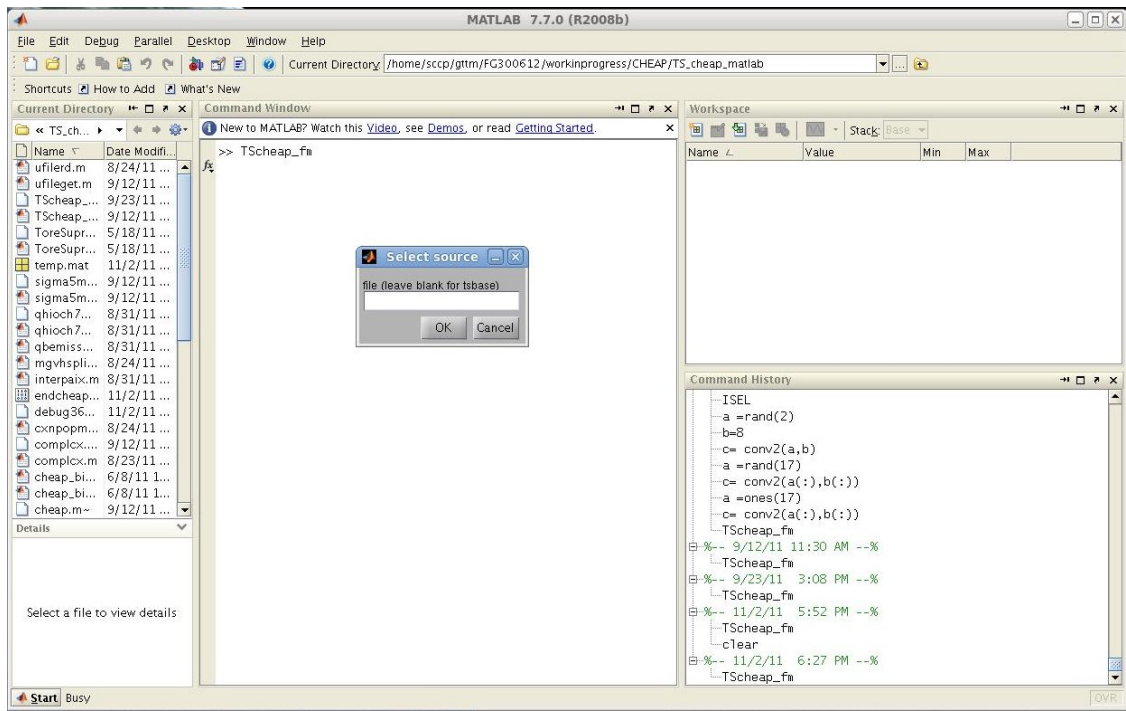
- New full MATLAB version of code CHEAP is available.
- Effective CX coefficients taken from ADAS database.
- Still under improving and developing.

# BACKUP SLIDES

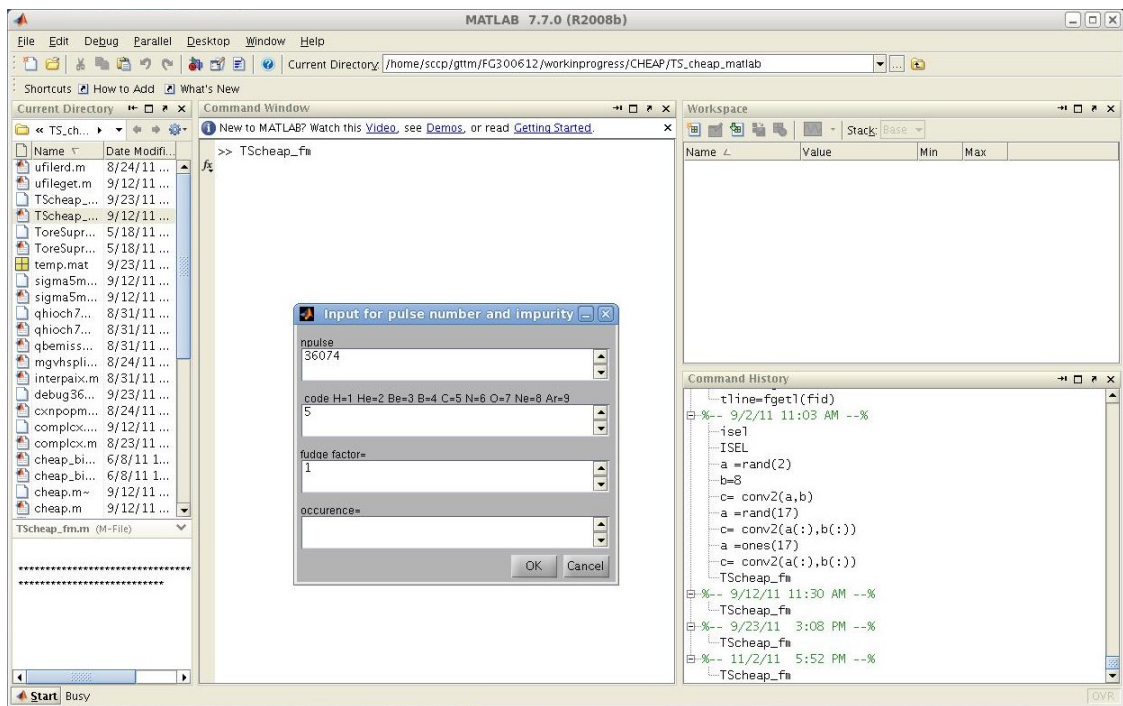
# Using CHEAP



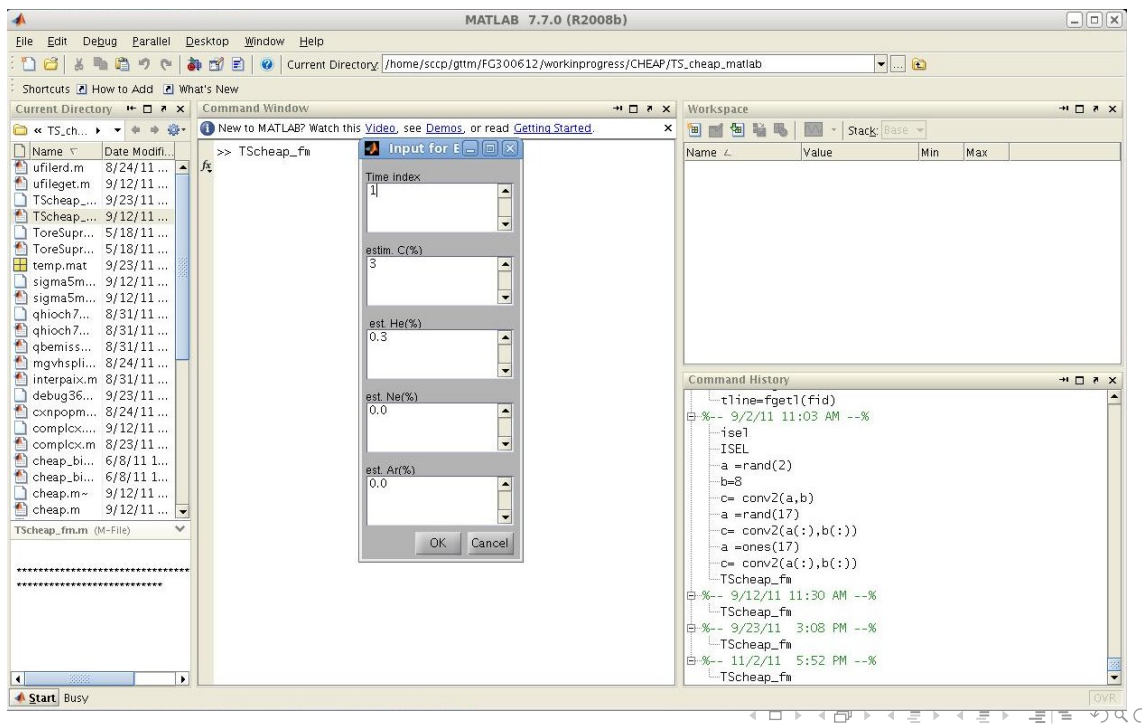
# Using CHEAP



# Using CHEAP

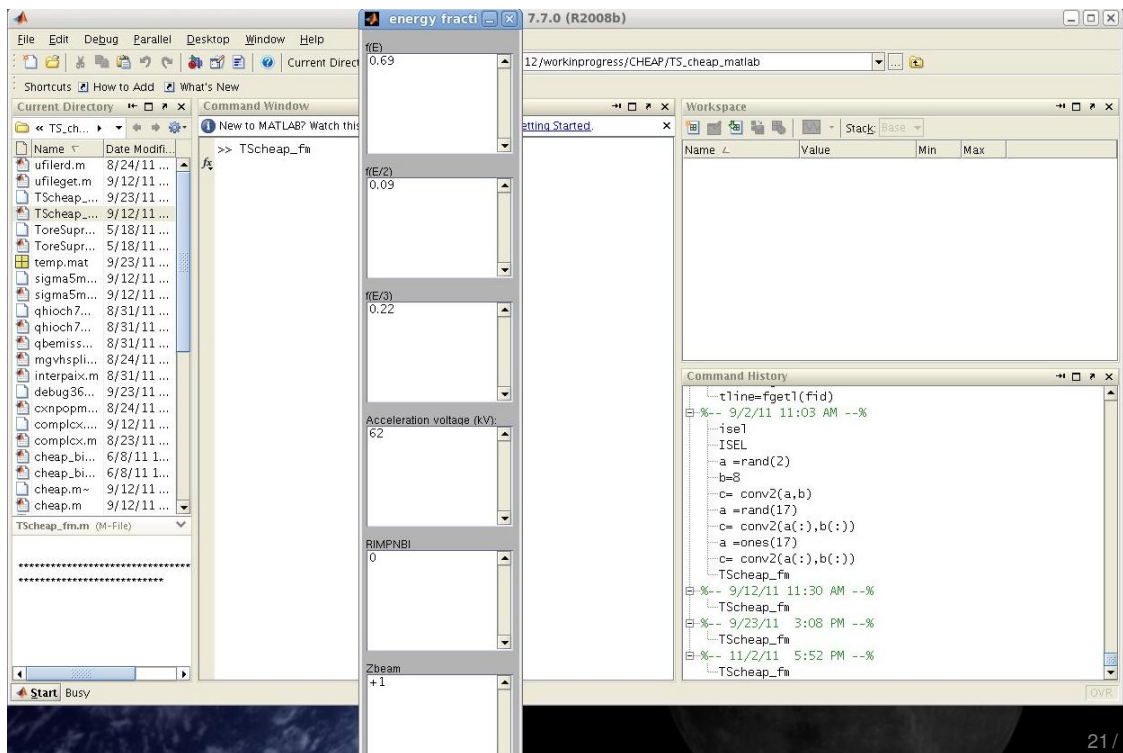


# Using CHEAP

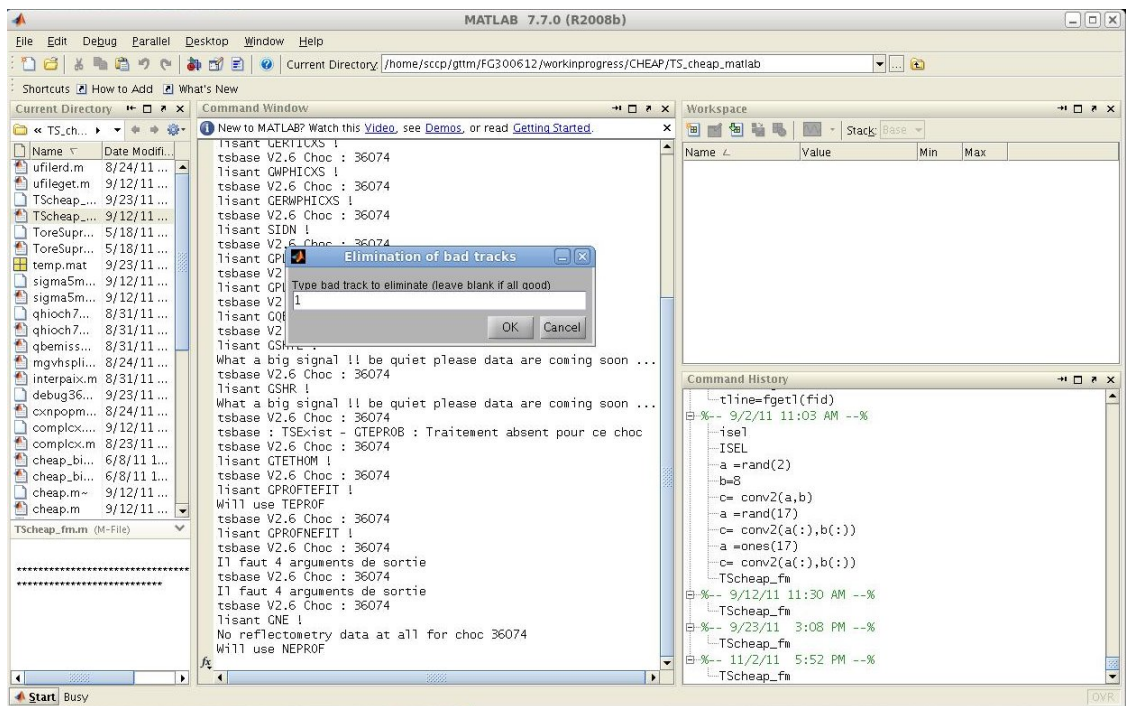




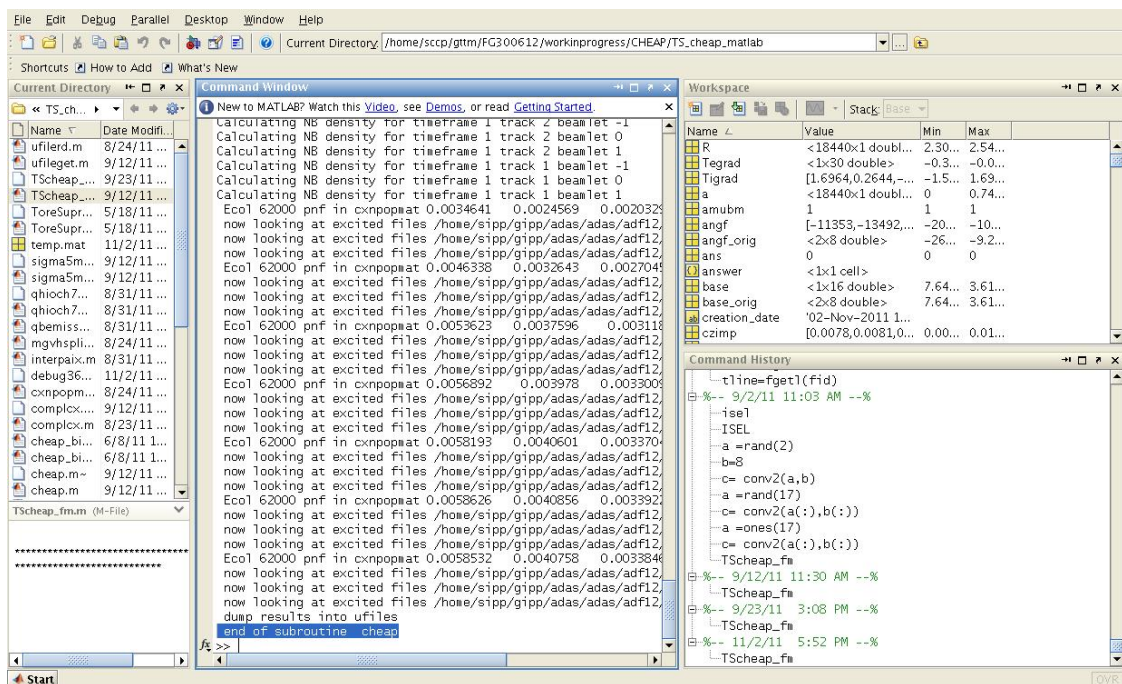
# Using CHEAP



# Using CHEAP



# Using CHEAP



-



## Appendix D

# Experimental quality assessment of Ar CX density profiles

### Experimental quality assessment of Ar CX density profiles.

**Date:** September 30, 2011

**Responsible Officer:** F. Guzmán<sup>1</sup>

**Co-Authors:** M. Sertoli<sup>2</sup>, R. McDermott<sup>3</sup>, R. Guirlet<sup>4</sup>, G. Mondet<sup>5</sup>

**Task Force:** V

**Preferred Date for Execution:** March 2012-April 2012

#### 1. Scientific Rationale

##### 1.1 Background

Argon is one of the impurities commonly injected in present-day magnetic fusion facilities for both physics purposes (impurity transport studies) and operation and safety purposes (edge radiation enhancement and heat flux reduction on the plasma facing components). It is also considered for ITER operation, where excessive heat fluxes will lead to damages and water leaks causing unacceptable delays in the scientific and technological programme.

Charge exchange recombination spectroscopy is the most direct technique to determine the argon density in a fusion plasma. This technique requires knowledge of the Ar charge-exchange (CX) cross-sections. Calculations of these quantities have been carried out by classical trajectory Monte Carlo methods (CTMC) using microcanonical [1] and hydrogenic distributions [2]. Microcanonical distributions are more adequate for the description of capture to low n-shells while hydrogenics describe better the capture to high n-shell [3, 4]. The new calculations of Ar cross-sections using an improved hydrogenic description of the initial distribution [5] (the previous sets come from calculation that used a microcanonical distribution [6]) have been released in ADAS [7]. A big discrepancy has been found between the different calculations reaching up to two orders of magnitude depending on the beam energy (see Fig. 1). Since the evaluation of the impurity density from charge-exchange recombination spectroscopy (CXRS) [8] depends directly on these cross-sections, such errors will lead to incorrect evaluations of the impurity density profiles.

##### 1.2 Goals

The quality of the CX cross-sections for argon 14+ to 18+ ionization stages will be studied by comparing argon density profiles evaluated through CXRS, using both cross-section data-sets, with those evaluated through the combined use of the soft-X Ray (SXR) diode array diagnostic and the Johann X-ray spectrometer. For the latter purpose we plan to use two independent codes [9, 10] in order to avoid biases due to the analysis method. In contrast to CXRS, the SXR diagnostic detects light emitted from recombined or electron-impact excited states and thus depends on independent sets of atomic data affected only by small uncertainties. Such a comparison will enable the detection of inconsistencies between electron impact and charge exchange data sets and allow us to evaluate the quality of the different CX atomic data-sets.

A preliminary comparison with the data from the Johann spectrometer only (M. Sertoli, private communication) suggested a good agreement with the new calculations [5] and a discrepancy of a factor  $\sim 20$  with older ones [6] (see Fig. 2), which come from a similar difference in the effective rates coefficients (see Fig. 3).

<sup>1</sup>ADAS-EU, U. Strathclyde

<sup>2</sup>IPP Garching

<sup>3</sup>IPP Garching

<sup>4</sup>CEA-Cadarache

<sup>5</sup>Laboratoire Aimé Cotton, Université Paris XI

## 2. Experiment details

Two CXRS diagnostics set on the same spectral line but viewing beams with different energies will enable us to study the relative effect of beam energy on the cross-section (CER on beam 3, CHR on beam 8) as well as make the absolute density comparison to the soft-X ray diagnostics. For each discharge, scans in ECRH power will be used to change the electron temperature profile and thus ensure optimal experimental conditions for the spectroscopic measurements and obtain good fractional abundance of the stage of ionization under study (see Fig. 4). Several discharges will be necessary in order to measure all of the relevant ionization stages.

### Global plasma parameters and additional heating

H-mode operation

$I_p = 0.8$  MA,  $Bt = -2.5$  T,  $P_{NBI} = 5 - 7.5$  MW,  $P_{ECH} = 0 - 4$  MW

Configuration: *LSN*

Gas: *D, Ar*

Beams 3 and 8 are compulsory for diagnostic purposes.

### Diagnostics Requirements

CHR, CER, CMR, BES, SXR, SIL, ECE, DCN, Li-beam, Core TS, Z-Effective, CPS

### Special Machine Requirements and Scare Resources

Divertor D fueling to ensure good CXRS measurements, Ar puffing, beam boxes 1 and 2, 3MW ECRH power

Number of successful discharges: 6

## References

- [1] R. Abrines and I. C. Percival. *Proc. Phys. Soc.*, 88: 861, 1966.
- [2] D. J. W. Hardie and R. E. Olson. *J. Phys. B: At. Mol. Phys.*, 16: 1983, 1983.
- [3] L. F. Errea, C. Illescas, L. Méndez, B. Pons, A. Riera, and J. Suárez. *Phys. Rev. A*, 70: 52713, 2004.
- [4] L. F. Errea, F. Guzmán, Clara Illescas, L. Méndez, B. Pons, A. Riera, and J. Suárez. *Plasma Physics and Controlled Fusion*, 48: 1585, 2006.
- [5] L F Errea, Clara Illescas, L Méndez, B Pons, A Riera, and J Suárez. *Journal of Physics B: Atomic, Molecular and Optical Physics*, 39(5): L91, 2006.
- [6] D. G. Whyte, R. C. Isler, M. R. Wade, D. R. Schultz, P. S. Krstic, C. C. Hung, and W. P. West. 5(10): 3694–3699, 1998.
- [7] H. P. Summers, 2007. Atomic Data and Analysis Structure User Manual.
- [8] C.F. Maggi, T. Pütterich, M. O'Mullane, H.P. Summers, C. Illescas, and M. von Hellermann. Experimental test of ar cross sections. In *ADAS Workshop, 2007*. Schloss Ringberg, Germany. 11–12 October.
- [9] M Sertoli, C Angioni, R Dux, R Neu, T Pütterich, V Igochine, and the ASDEX Upgrade Team. *Plasma Physics and Controlled Fusion*, 53(3): 035024, 2011.
- [10] T Parisot, R Guirlet, C Bourdelle, X Garbet, N Dubuit, F Imbeaux and PR Thomas. *Plasma Physics and Controlled Fusion*, 50: 055010, 2008.

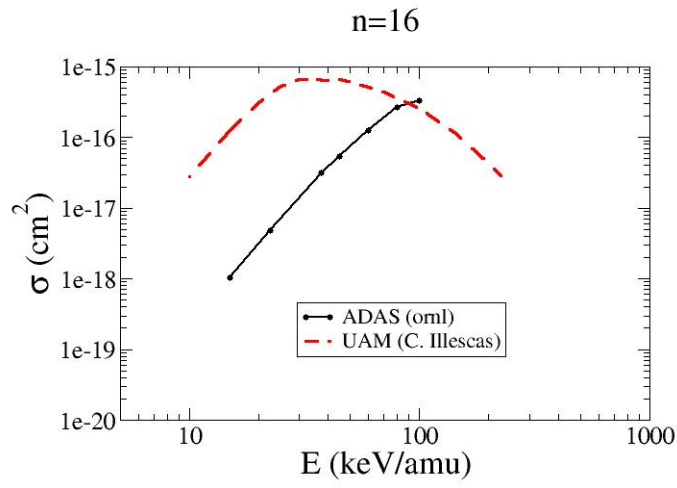


Figure 1: Ar18+ + H(1s) capture to n=16 cross section comparison between ORNL calculations[6] and new UAM calculations[5].



Shot = 22305 Time = 2.650 s

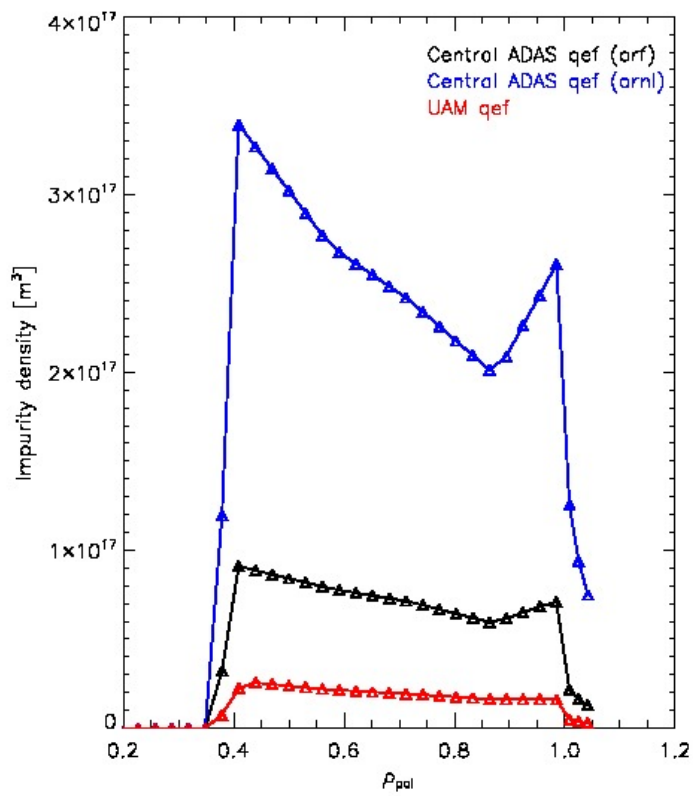


Figure 2: Density profile for ArXVI in ASDEX-U from ORNL[6] (blue) and UAM[5] (red) data versus poloidal radius. Black profile come from a interpolation averaging between these two sets[7].

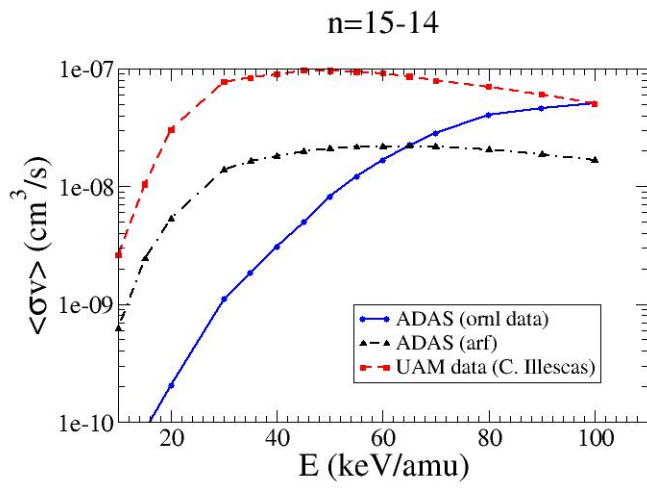


Figure 3:  $\text{Ar}^{16+} + \text{H}(1s)$  effective coefficients for the transition  $n = 15 - n = 14$  comparison between ORNL calculations[6] and new UAM calculations[5]. "ARF" profile come from a interpolation averaging between these two sets[7]

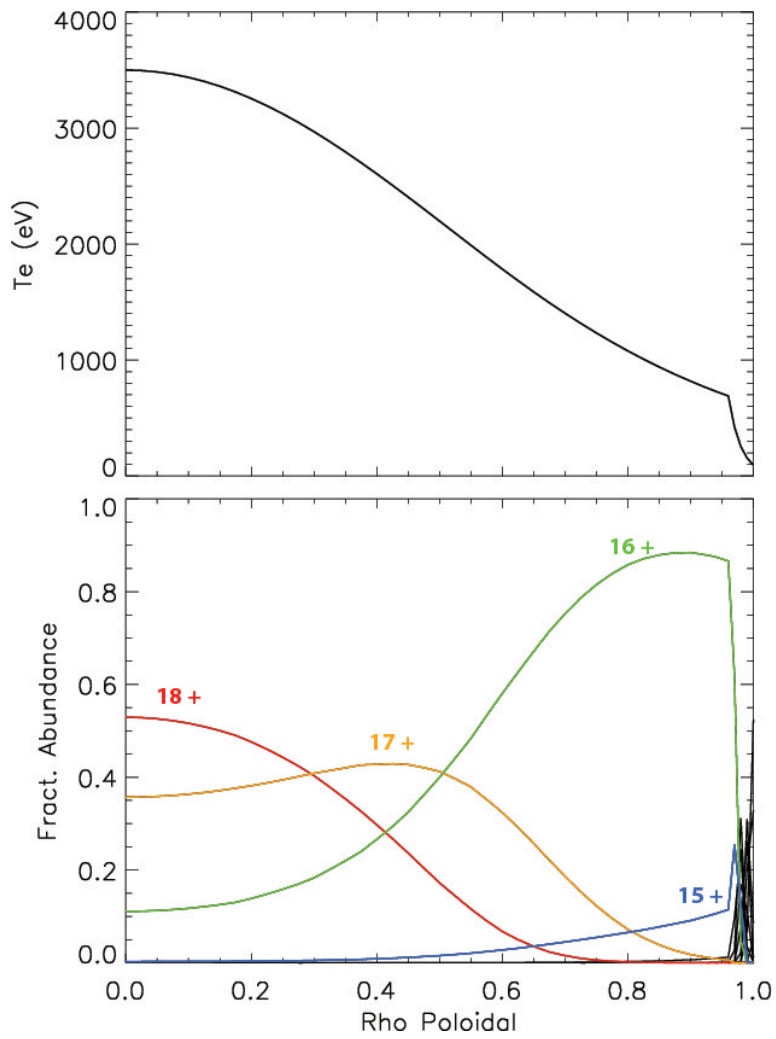


Figure 4: Variation of fractional abundance of Ar ionization stages with poloidal radius as electronic temperature is increasing towards the plasma core.

-



## Appendix E

# ADAS-EU travel report: ITM workshop Cyprus 3-13 October

### ADAS-EU Travel Report

*Location:* Nicosia University, Cyprus.  
*Date:* 3-13 Octobre 2011.  
*ADAS-EU staff:* Francisco Guzman  
*Purpose:* ITM Code Camp

*Items:*

- (1) Discussion of the molecular data needing from AMNS project
- (2) Discussion of progress in the ADAS-EU molecular data and collisional-radiative modelling.
- (3) Discussion of involvement of ADAS-EU staff in AMNS project.
- (4) Planning and scheduling of deadlines for delivering of data.

*AMNS molecular data:*

- (5) The first session consisted in the introduction of Francisco Guzmán to the AMNS members. Before that FG familiarized with the working way of ITM and acceded to its documentation.
- (6) First discussions about molecular data with D. Coster and D. Tskakhaya. FG explained that ADAS molecular model will allow AMNS to store effective coefficients in CPOs and cross section data and it may be needed others parameters as vibrational energies etc.
- (7) Discussion about possible new ionization data with K. Tokesi where carried out.
- (8) Data needs from AMNS were defined in a separate meeting session and a first document (attached) was produced with the requirements from AMNS. Molecular ADAS will be able to provide molecular effective coefficients in mdf11 format for diatomic molecules in the required energy range for which data exist and specially for H<sub>2</sub> and its isotopes.

*ADAS-EU involvement:*

- (9) As ADAS900 series data are very useful for AMNS project, it was agreed that data format files and reading routines will be free access as usual in ADAS and FG would provide support for reading the files and the correct use of them during year 2012 when a complete working version of the Molecular Collisional Radiative Model is finish.
- (10) FG will participate in future Code Camps to facilitate this support during the next year.

F. Guzmán  
25 October 2011

-